

## Solifluction Processes on Permafrost and Non-permafrost Slopes: Results of a Large-scale Laboratory Simulation

Charles Harris,<sup>1\*</sup> Martina Kern-Luetsch,<sup>1†</sup> Julian Murton,<sup>2</sup> Marianne Font,<sup>3</sup> Michael Davies<sup>4</sup> and Fraser Smith<sup>5</sup>

<sup>1</sup> School of Earth and Ocean Sciences, Cardiff University, Cardiff, UK

<sup>2</sup> University of Sussex, Department of Geography, Brighton, UK

<sup>3</sup> Laboratoire M2C, Université de Caen-Basse Normandie, Centre National de la Recherche Scientifique, France

<sup>4</sup> Faculty of Engineering, University of Auckland, Auckland, New Zealand

<sup>5</sup> School of Engineering, University of Dundee, Dundee, UK

### ABSTRACT

We present results of full-scale physical modelling of solifluction in two thermally defined environments: (a) seasonal frost penetration but no permafrost, and (b) a seasonally thawed active layer above cold permafrost. Modelling was undertaken at the Laboratoire M2C, Université de Caen-Basse Normandie, Centre National de la Recherche Scientifique, France. Two geometrically similar slope models were constructed using natural frost-susceptible test soil. In Model 1 water was supplied via a basal sand layer during freezing. In Model 2 the basal sand layer contained refrigerated copper tubing that maintained a permafrost table. Soil freezing was from the top down in Model 1 (one-sided freezing) but from the top down and bottom up (two-sided freezing) in Model 2. Thawing occurred from the top down as a result of positive air temperatures. Ice segregation in Model 1 decreased with depth, but in Model 2, simulated rainfall led to summer frost heave associated with ice segregation at the permafrost table, and subsequent two-sided freezing increased basal ice contents further. Thaw consolidation in Model 1 decreased with depth, but in Model 2 was greatest in the ice-rich basal layer. Soil shear strain occurred during thaw consolidation and was accompanied by raised pore water pressures. Displacement profiles showed decreasing movement rates with depth in Model 1 (one-sided freezing) but 'plug-like' displacements of the active layer over a shearing basal zone in Model 2 (two-sided active layer freezing). Volumetric transport rates were approximately 2.8 times higher for a given rate of surface movement in the permafrost model compared with the non-permafrost model. Copyright © 2008 John Wiley & Sons, Ltd.

KEY WORDS: solifluction; physical modelling; permafrost; seasonally frozen ground

### INTRODUCTION

In this paper we compare solifluction processes observed in two large-scale laboratory physical models that had identical slope geometries and soil

characteristics, but contrasting thermal regimes. Model 1 was subject to cycles of freezing and thawing from the surface to the base (simulating seasonally frozen ground), while in Model 2 a permafrost table was maintained at the base and active layer thaw/freeze was simulated with a thaw front penetrating from the surface downwards to the permafrost table, followed by freezing from the surface downwards and from the permafrost table upwards (two-sided freezing) (see Harris *et al.*, 2008b). These experiments were run in parallel with scaled centrifuge physical

\* Correspondence to: Charles Harris, School of Earth and Ocean Sciences, Main Building, Park Place, Cardiff University, Cardiff, CF10 3YE UK. E-mail: harrisc@cardiff.ac.uk

† Current address: WSL Institute for Snow and Avalanche Research SLF, Davos, Switzerland.

modelling experiments (Kern-Luetsch *et al.*, 2008; Kern-Luschg and Harris, 2008) and validated against field studies in Dovrefjell, Norway (seasonally frozen) and Svalbard (continuous permafrost) (Harris *et al.*, 2006, 2008c). Resulting data will allow detailed assessment of cryogenic soil processes, and provide validation and calibration for on-going numerical modelling (Cleall *et al.*, 2006; Thomas *et al.*, submitted).

## SOLIFLUCTION PROCESSES

Where soils are moist and frost-susceptible, winter frost penetration causes ice segregation and frost heave, and subsequent summer thaw leads to surface resettlement, and on sloping ground, downslope soil displacements by solifluction (gelifluction and/or frost creep) (e.g. Washburn, 1967; Benedict, 1970; Harris, 1981; Smith, 1988; Matsuoka, 2001; Kinnard and Lewkowicz, 2005; Jaesch *et al.*, 2003). Ice contents in the frozen soil and downslope displacements during thaw both often decrease with depth. Harris and Davies (2000) argued that both cryogenic suction and heaving pressure increase with depth during ice segregation, and lead to progressively greater over-consolidation and undrained shear strengths within the soil matrix. This tends to limit solifluction on seasonally frozen slopes to the uppermost 50 cm or so of soil. In cold permafrost regions, however, two-sided active layer freezing (Mackay, 1981; Cheng, 1983; Lewkowicz and Clarke, 1998; Shur, 1988; Shiklomanov and Nelson, 2007) commonly leads to ice segregation at the base of the active layer and top of the permafrost, forming an ice-rich 'transient layer' (Shur *et al.*, 2005). Active layer solifluction movements are observed mainly in late summer when melting of the ice-rich basal zone is in progress (Lewkowicz and Clarke, 1998; Matsuoka and Hirakawa, 2000). Mackay (1981, 1983) showed that ice within this zone forms by early winter upward advance of a freezing front from the permafrost table, augmented in late summer by refreezing of water migrating downwards across the thaw front and into still-frozen basal active layer and upper permafrost.

## PRINCIPAL AIMS OF THE PRESENT RESEARCH

The experiments described here involved half-hourly measurements of soil temperatures, surface frost heave, thaw settlement, pore water pressure and downslope displacements, on two slopes with surface

gradients of 12° constructed of the same experimental soil. The principal aims were to test the following hypotheses:

The distribution of segregation ice and the timing of frost heaving and resettlement differ in seasonally frozen ground (one-sided freezing) and seasonally thawed active layers above cold permafrost (two-sided freezing).

The distribution of shear strain during thaw is closely related to the distribution of both segregation ice and thaw consolidation within the soil profile.

Pore pressures are raised during thaw consolidation of ice-rich soil, leading to a reduction in effective stress and incremental shear deformations.

## PHYSICAL MODELLING

Laboratory experimentation to simulate slope processes within thawing fine-grained soils offers a number of advantages over equivalent field studies, including the ability to control environmental parameters, precise definition of experimental boundary conditions, the potential for more detailed and complex data collection, and the capability to reduce the time scale of freeze-thaw cycling, allowing many years of field processes to be modelled in a relatively short time period (Harris, 1996). Since the early experiments of Higashi and Corte (1971), physical modelling of solifluction has focused almost entirely on slopes with one-sided soil freezing and no permafrost. Higashi and Corte explored the relationship between slope angle, frost creep and needle ice formation, while larger scale simulations by Journaux and Coutard (1976), Coutard *et al.* (1988) and Harris *et al.* (1993) investigated the distribution of shear strain with depth, the significance of soil granulometry, and the relative importance of frost creep and gelifluction. Frost creep has been shown to be more important in coarser soils containing less silt and clay, while gelifluction dominates where soils are richer in fines. Papers by Harris *et al.* (1995, 1997, 2008b) and Harris and Davies (2000) have shown that solifluction movements occur during thaw settlement when pore pressures are raised. Two-dimensional (2-D) vectors of surface movement due to frost heave, thaw settlement and downslope displacement, collected during laboratory simulations of one-sided soil freezing, have been shown to resemble field measurements in Greenland (Washburn, 1967, 1979) and Norway (Harris *et al.*, 2008c).

Virtually the only full-scale laboratory simulation experiment specifically investigating the significance of ice distribution within thawing soils was reported

by Rein and Burrous (1980) who used a tilting box containing a 25 cm thick layer of frost-susceptible silt-loam. Two experiments were conducted, firstly with high ice contents in the mid profile, the second with high ice contents at the base. Thaw consolidation and solifluction were shown to be concentrated within these ice-rich layers, with little shear strain occurring elsewhere in the profile.

In a second methodological approach to physical modelling, Harris *et al.* (2000, 2001, 2002) undertook reduced scale modelling under elevated gravitation fields in a geotechnical centrifuge using the same silt-rich test soils as were used in earlier full-scale experiments. Centrifuge modelling successfully simulated solifluction movements associated with one-sided freezing, and a consideration of scaling issues showed that shear strain within the thawing soils reflected the elasto-plastic response of a frictional material rather than the slow flow of a viscous liquid (Harris *et al.*, 2003). Simulations using a range of soil types (Harris *et al.*, 2008a) also demonstrated changes in the depth distribution of shear strain, with non-cohesive silt-rich soils associated with maximum shear strain near the surface, giving strongly concave downslope profiles of movement, and more cohesive clay-rich soils showing maximum shear strain at depth, giving convex downslope profiles.

## EXPERIMENTAL DESIGN

In the experiments reported here, two slope models were constructed adjacent to each other within a 5 m × 5 m freezing chamber (Figures 1 and 2) using a natural frost-susceptible silt-rich soil collected from Normandy, France. Soil properties are summarised in Table 1. Each model was 5 m long, 1.5 m wide and 350 mm thick (Harris *et al.*, 2008c). The soil is considered similar to many non-cohesive solifluction soils reported in the literature (see for instance the review by Harris, 1981). Model 1, simulating one-sided seasonal freezing and thawing, was constructed above a sand basal layer through which water was supplied during freezing, maintaining an open system (Figure 1b). Variation in frost heaving during successive freezing cycles was achieved by varying the rate of water supply.

In contrast, Model 2 (active layer subjected to two-sided freezing followed by thawing from the surface downwards, overlying permafrost) was constructed above refrigerated copper tubing embedded in a layer of sand (Figure 1b), which allowed a basal layer to be maintained at a temperature of  $-2.0 \pm 0.5^\circ\text{C}$ . Thus, the lowermost 40 mm of model soil plus the

underlying sand layer remained permanently frozen. Since the maximum thaw depth was only around 310 mm, active layer thickness was much less than in most field situations. Air temperatures above both model slopes were lowered to between  $-8^\circ\text{C}$  and  $-12^\circ\text{C}$  to simulate winter freezing, and were subsequently raised to between  $+15^\circ\text{C}$  and  $+20^\circ\text{C}$  to simulate the summer thaw period. Moisture contents prior to initiation of winter freezing averaged around 25 per cent by weight in the two-sided freezing model, but were slightly higher in the one-sided model.

## INSTRUMENTATION

Figure 1 shows the location of instrumentation. All data were collected at half-hourly intervals via a PC-based logging system. Temperatures were monitored using an array of stainless steel thermistor probes measuring to within  $\pm 0.38^\circ\text{C}$ , supplied by Campbell Scientific Ltd., Loughborough, UK installed in mid-slope locations at the surface and depths of 0, 50, 150, 250 and 350 mm in Model 1 (one-sided freezing), and 0, 50, 150, 250, 300 and 350 mm in Model 2 (two-sided freezing). Pore water pressures were measured using Druck Ltd., Wolverhampton, UK PDCR 81 miniature pore pressure transducers consisting of stainless steel cylinders of diameter 6 mm and length 12 mm with a porous stone tip. Transducers were filled with low viscosity silicon oil, and had a range of 350 mb, combined non-linearity and hysteresis of  $\pm 0.2$  per cent and thermal sensitivity of 0.2 per cent of reading per  $^\circ\text{C}$  and were installed alongside thermistor probes at depths of 50, 150 and 250 mm in Model 1, and 150, 250 and 300 mm in Model 2.

Soil surface motion was recorded using pairs of longstroke (300 mm) captive guided armature linear variable differential transformers (LVDTs) supplied by RDP Electronics Ltd., Wolverhampton, UK, with spherical end bearings. Pairs of LVDTs formed a fixed base triangle mounted on a slotted track parallel to the slope above each model, supported by a beam (Figure 1). Both LVDTs were connected to an 80 mm × 80 mm Perspex footplate embedded in the soil surface, forming the apex of the triangle (Figure 1b). Frost heave, thaw consolidation and downslope displacements of the soil surface were registered by changes in LVDT length, and were resolved as orthogonal vectors perpendicular and parallel to the soil surface to an estimated accuracy of  $\pm 1.5$  mm (see Harris *et al.*, 1996 for details). Soil displacement profiles were observed through re-excavation of Rudberg columns comprising 10 mm long sections of plastic tubing of external diameter 15 mm. Sections were threaded over

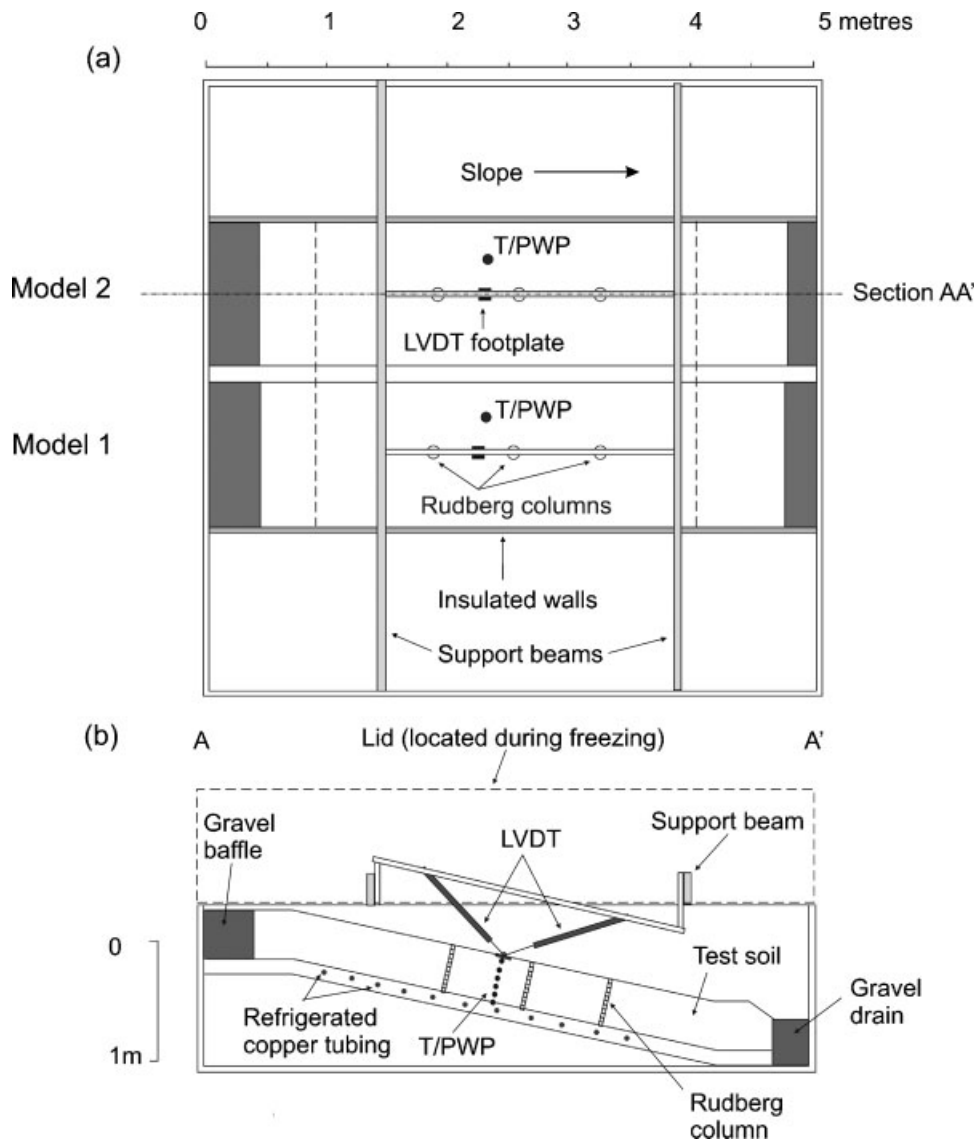


Figure 1 Experimental slopes showing instrumentation. (a) Plan. (b) Section A-A' through two-sided freezing model (Model 2). Note refrigerated tubing embedded within sand forming the basal refrigeration plate. In the one-sided freezing model (Model 1) no refrigeration tubes are present, but a constant head water supply is introduced to the basal sand at the top of the slope (left side of figure) via pipe work passing through the container walls. T/PWP = Thermistors and pore pressure transducers; LVDT = linear variable differential transformer.

a steel rod to form column lengths 40 cm, and these were pushed into a hole augured from the surface to the basal sand. The steel rod was then withdrawn, leaving column sections free to move with the soil.

### EXPERIMENTAL PROCEDURE

Cyclical soil freezing and thawing commenced in February 2005 and ended in September 2007. To

initiate the freeze/thaw cycles, moisture contents in both models were raised by introducing a constant head supply of water into the basal sand layers of each slope. In both cases gravimetric moisture content ranged from around 25 per cent near the slope crest to 28 per cent in the footslope zone. Maintaining an open water supply to the basal sand layer, both models were initially frozen from the surface downwards by lowering air temperatures to around  $-10^{\circ}\text{C}$ . When



Figure 2 Slope models at the end of a thawing phase, immediately before re-location of freezing container lid prior to lowering air temperatures above the models to initiate the next freezing phase. Model 2 (two-sided freezing with permafrost) far side, Model 1 (one-sided freezing, no permafrost) near side.

Table 1 Average test soil properties

% clay	% silt	% sand	PL %	LL %	$\phi$ degrees	$c_v$ m <sup>2</sup> /yr	k m/s
25	65	10	22	33	26	18.4	$4.4 \times 10^{-8}$

PL = Plastic limit; LL = liquid limit;  $c_v$  is coefficient of consolidation; k = permeability.

frozen, the basal refrigeration unit was activated in Model 2 (permafrost) and the thermostat was set to maintain a permafrost table at a maximum depth of 310 mm during each thaw stage. In Model 1 (seasonal frost) the test soil and the underlying basal sand layer were frozen completely during each freezing cycle, with an open water supply maintained to the sand layer. The model was allowed to thaw completely during successive thaw cycles.

During each simulated summer period, at the stage when the active layer in Model 2 was close to its maximum depth, water was introduced to the surface using a fine spray. In most cycles 15 l of water were added in increments of 5 l over a period of several days. This was equivalent to around 3.5 mm simulated

rainfall. Downward percolation led to re-hydration of the active layer and migration of water to the permafrost table where refreezing led to significant summer frost heave. Unfortunately, problems with the refrigeration unit led to non-uniform basal cooling and spatially variable frost heaving during the initial eight freeze-thaw cycles. The system was overhauled in May 2006 and new Rudberg columns installed. A second series of eight freeze-thaw cycles was then initiated, as described above, and during these, Model 2 basal temperatures were spatially uniform and the permafrost table was planar. All direct comparisons between the two model slopes presented below refer to the second series of eight freezing and thawing cycles, between May 2006 and August

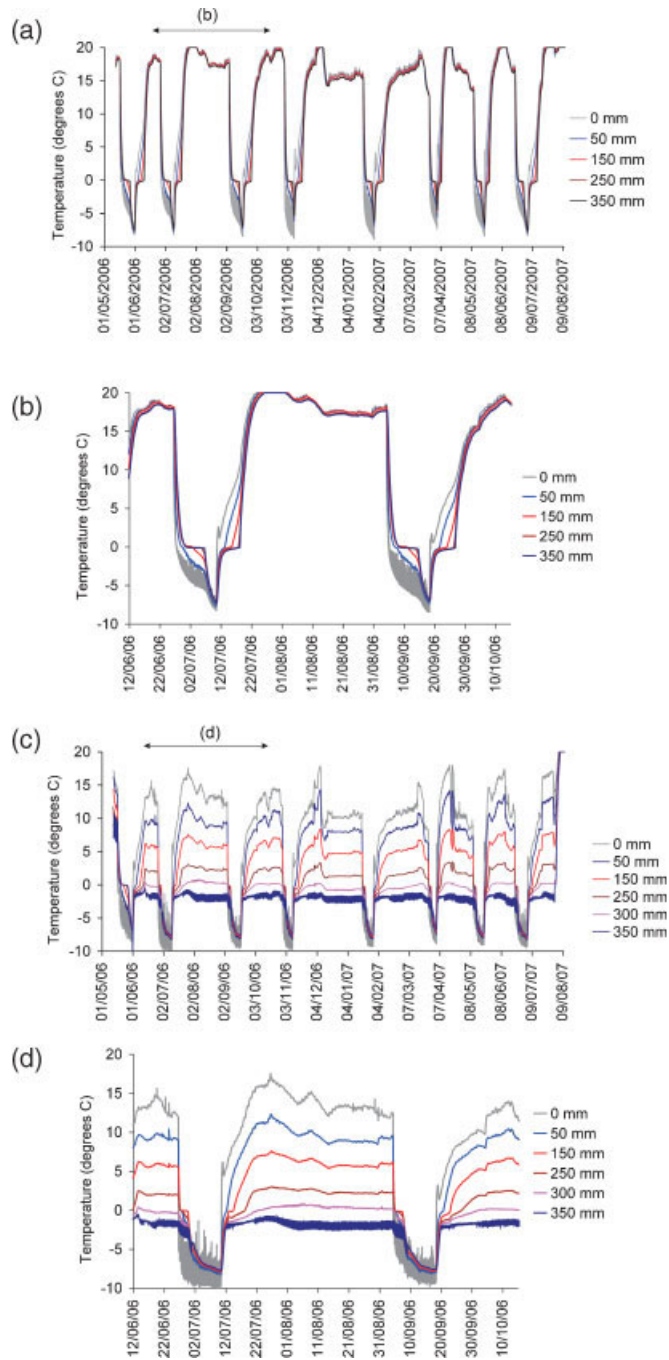


Figure 3 Temperature time series. (a) Model 1, cycles nine to 16 (one-sided freezing, no permafrost). Bar labelled (b) shows time period shown in 3b. (b) Model 1, detail, cycles ten and 11. (c) Model 2, cycles nine to 6 (two-sided freezing, permafrost). Bar labelled (d) shows time period shown in 3d. (d) Model 2, detail, cycles ten and 11.

2007. However, since Model 1 (one-sided freezing simulating seasonally frozen ground) functioned well throughout all the 16 cycles of the experiment, data collected in the earlier phase are also presented in the analysis of some process variables.

## RESULTS

### Soil Temperatures

The time series of soil temperatures during cycles nine to 16 are shown in Figure 3a and 3c, and in more detail for cycles ten and 11 in Figure 3b and 3d. Penetration of both the freezing and thawing fronts was accompanied by a more prolonged zero curtain effect in Model 1 (surface downwards freezing and no permafrost) than was the case in Model 2, reflecting unidirectional rather than bidirectional heat conduction. Identification of the time and date when phase change was complete at each monitored depth allowed penetration of freezing and thawing fronts to be determined, and examples from cycles ten and 11 are shown in Figure 4. Freezing rates were significantly slower in Model 1 than in the Model 2, with average duration of freezing 198 h in Model 1 and 67 h in Model 2.

Upward advance of the freezing front from the permafrost table in Model 2 was initiated by the fall in upper boundary temperature that began each freezing cycle. Upward and downward thermal gradients were accompanied by converging freezing fronts, the active layer acting as a closed hydraulic system. Thus any migration of water towards the freezing fronts would have left the central part of the active layer starved of

moisture, and ice contents here were, in consequence, low. In Model 1 the rate of frost penetration increased significantly below 250 mm unfrozen depth, suggesting a decrease in ice segregation and hence a reduction in latent heat release. It is likely that the water supply was cut off as freezing approached the model base due to freezing of the supply pipes.

### Frost Heave, Thaw Settlement and the Distribution of Ice within the Frozen Soil

Frost heave perpendicular to the slope surface was determined by resolving changes in LVDT lengths using the simple trigonometry of the fixed base triangle (see Harris *et al.*, 1996). Typical heave and resettlement time series are provided by cycles ten and 11, illustrated in Figure 5. In Model 1 (one-sided freezing), frost heaving and thaw settlement accompanied penetration of the freezing and thawing fronts, giving a simple cyclical sequence. Total frost heave values in Model 1 varied (see Figure 6) in response to variations in basal water supply. In the permafrost model (Model 2), significant 'summer frost heaving' followed simulated summer rainfall (Figure 5) and subsequent 'winter' active layer freezing associated with sub-zero air temperatures took place in a closed hydraulic system, unlike Model 1.

Since soil freezing in Model 2 was from the top down and from the bottom upwards, it was not possible to determine precisely where ice segregation occurred during freezing. However, using the thermal data to determine the timing and duration of thaw through successively deeper soil layers, and assuming that

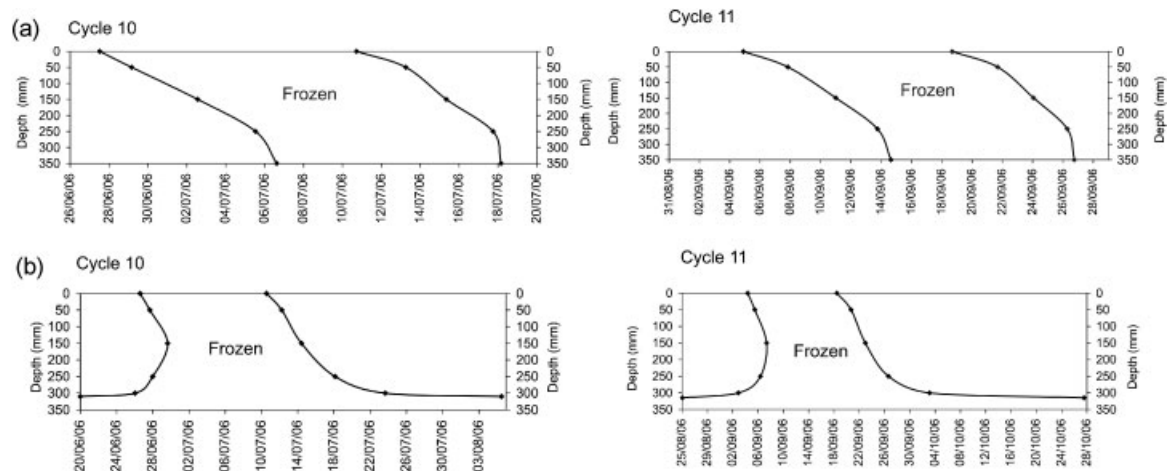


Figure 4 Penetration of freezing and thawing fronts, cycles ten and 11. (a) Model 1. (b) Model 2.

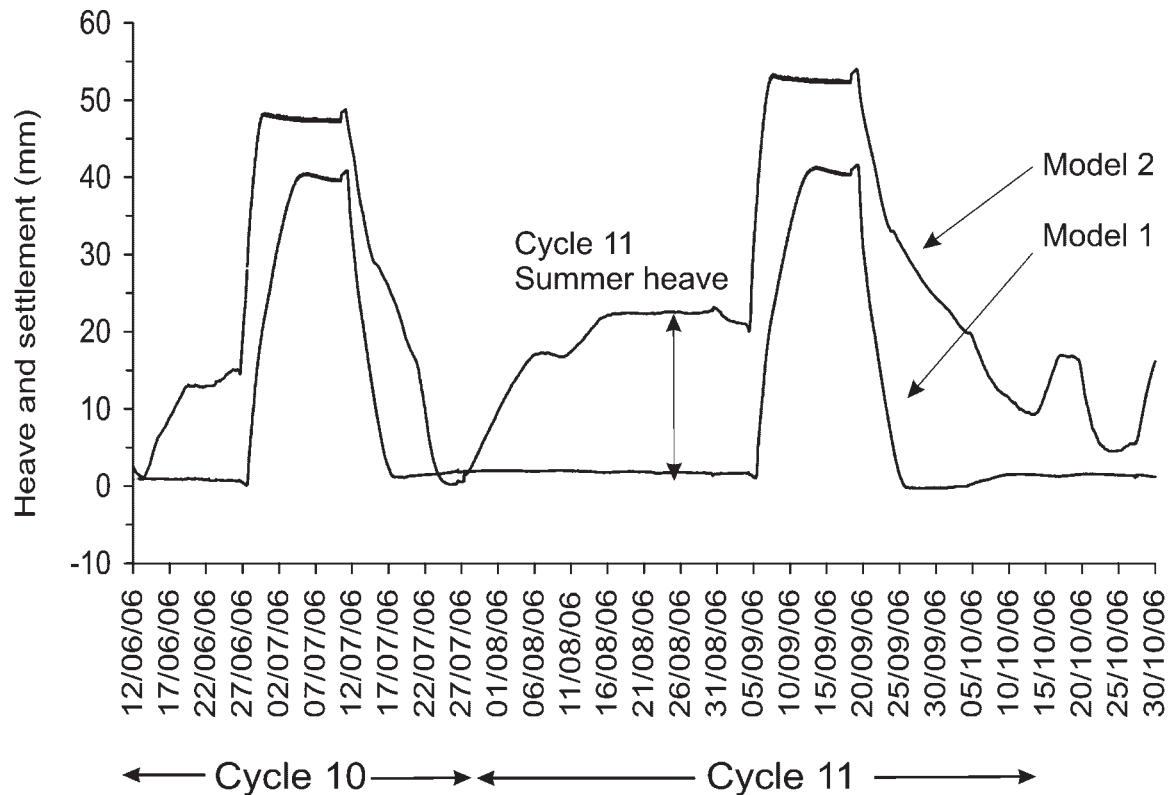


Figure 5 Typical patterns of heave and resettlement, cycles ten and 11.

recorded surface settlement over a given time period reflected thaw consolidation within the layer that thawed over the same time period, we were able to estimate the distribution of soil ice in each thawing cycle (Table 2) by calculating heaving ratios equivalent to the observed thaw consolidation, where heaving ratio is defined as the amount of heave (or in this case thaw settlement) within a given soil layer divided by the frozen thickness. This, however, ignored any settlement that may have taken place due to soil drying following thaw, so represents the maximum possible ice content values. Clearly, ice segregation was greatest within the uppermost 50 mm of Model 1, and decreased with depth, while in Model 2, summer heave plus downward migration of water during two-sided freezing contributed to a significant increase in ice content within the basal layer. In Model 2, the central part of the active layer showed relatively low ice contents.

### Thaw Settlement and Downslope Soil Movements

Time series of downslope surface movement and thaw settlement, as measured by displacement of the

LVDT surface footplate, are illustrated in Figure 6. Downslope surface movement in Model 1 (one-sided freezing) occurred during surface settlement caused by melting of excess soil ice and expulsion of meltwater (thaw consolidation, McRoberts and Morgenstern, 1974). In Model 2, surface movement patterns were more complex, with surface movement accompanying initial thaw of the near-surface soil layers, irregular slight upslope and downslope soil movements during thaw of the mid-zone of the active layer, followed by a second phase of downslope movement recorded during later thawing of the basal ice-rich zone. Again, solifluction movements were always associated with thaw consolidation.

Combining soil surface movements perpendicular and parallel to the gradient allowed a 2-D vector of the surface to be constructed (Figure 7). Vector shapes for the one-sided experiment were consistent during successive cycles, with simple one-stage heave during freezing (stage 1 in the interpretation of Model 1, Figure 7a), followed by thaw, leading initially to relatively rapid surface displacements with high ratios of displacement/thaw settlement (stage 2, Figure 7a)

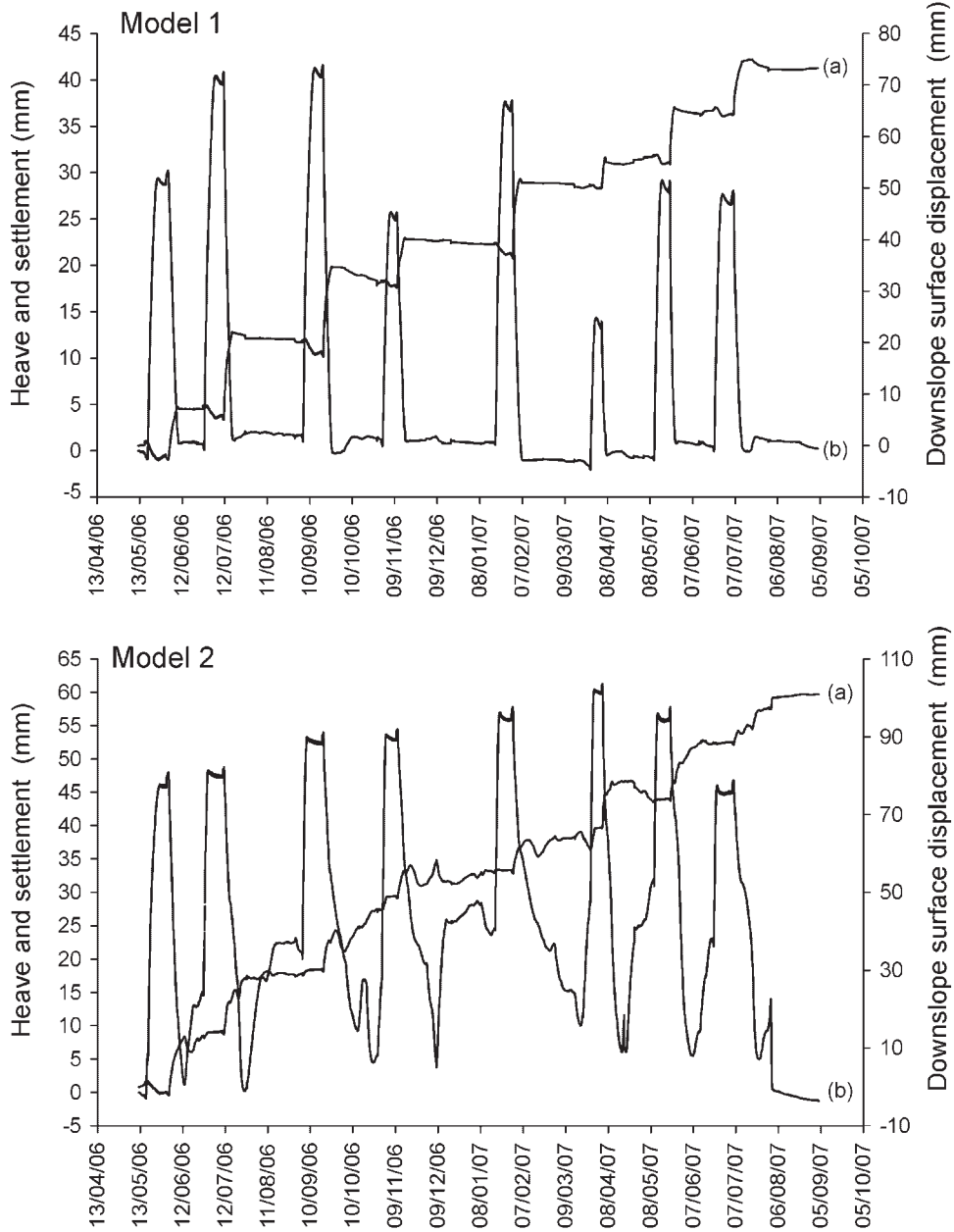


Figure 6 Record of heave and resettlement and associated downslope surface displacements, cycles nine to 16.

Table 2 Mean heaving ratios: Models 1 and 2, cycles ten to 16

Depth Model 1 (mm)	Model 1 Mean heaving ratio	Depth Model 2 (mm)	Model 2 Mean heaving ratio
0–50	0.26	0–50	0.13
50–150	0.11	50–150	0.08
150–250	0.04	150–250	0.06
250–350	0	250–300	0.24
		300–310	0.45

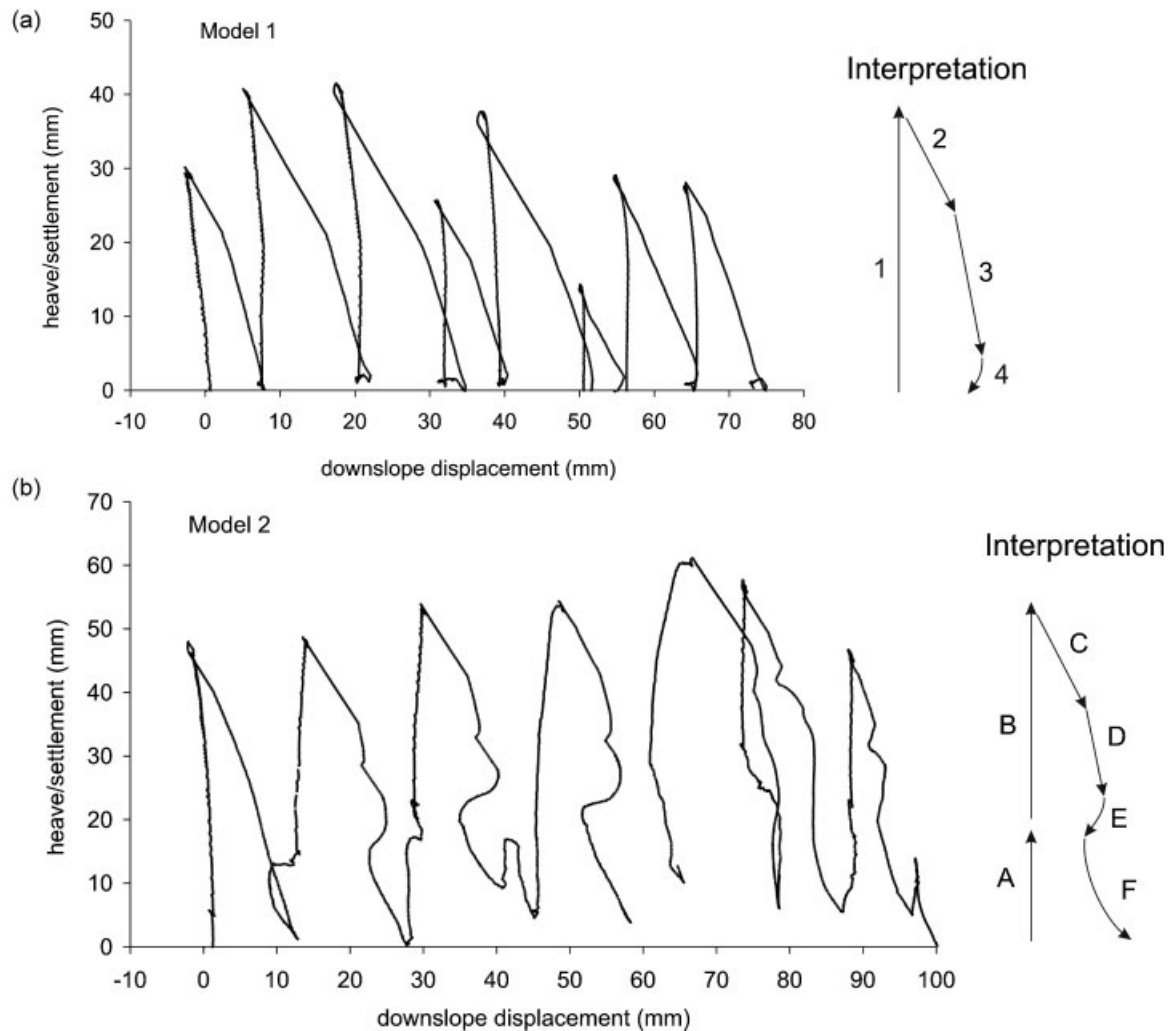


Figure 7 Vectors of surface movement, cycles nine to 16. (a) Model 1. (b) Model 2. In Model 2, the vector for cycle nine, which initiated the simulation sequence, is equivalent to the one-sided freezing cycles shown in (a) for Model 1 (see text for explanation). Cycle 13 has been omitted since irregular and complex footplate displacements were recorded associated with non-constant thermal boundary conditions and drying of the soil during that cycle. See text for explanation of the interpretation diagrams.

and subsequently somewhat lower displacement/thaw settlement ratios (stage 3, Figure 7a) as thawing progressed downwards. In some cycles, a final small retrograde movement was observed, thought to result from drying of the slope model (stage 4, Figure 7a). The two-sided experiment showed some variation on a pattern of summer heave caused by basal ice segregation (A, Figure 7b), winter heave as surface temperatures were lowered (B, Figure 7b), downslope displacements associated with thawing of the near-surface and upper mid part of the active layer (C and

D, Figure 7b), marked retrograde movement as the lower mid active layer thawed and soil drying took place (E, Figure 7b), and finally late summer movement associated with basal shearing as the ice-rich basal zone thawed (F, Figure 7b).

It should be noted that in Model 2, the series of freeze-thaw cycles was initiated in cycle nine by freezing from the surface downwards until the model was completely frozen, before the basal freezing unit was activated. Thus cycle nine in Model 2 represents one-sided freezing, and the vector shape is more

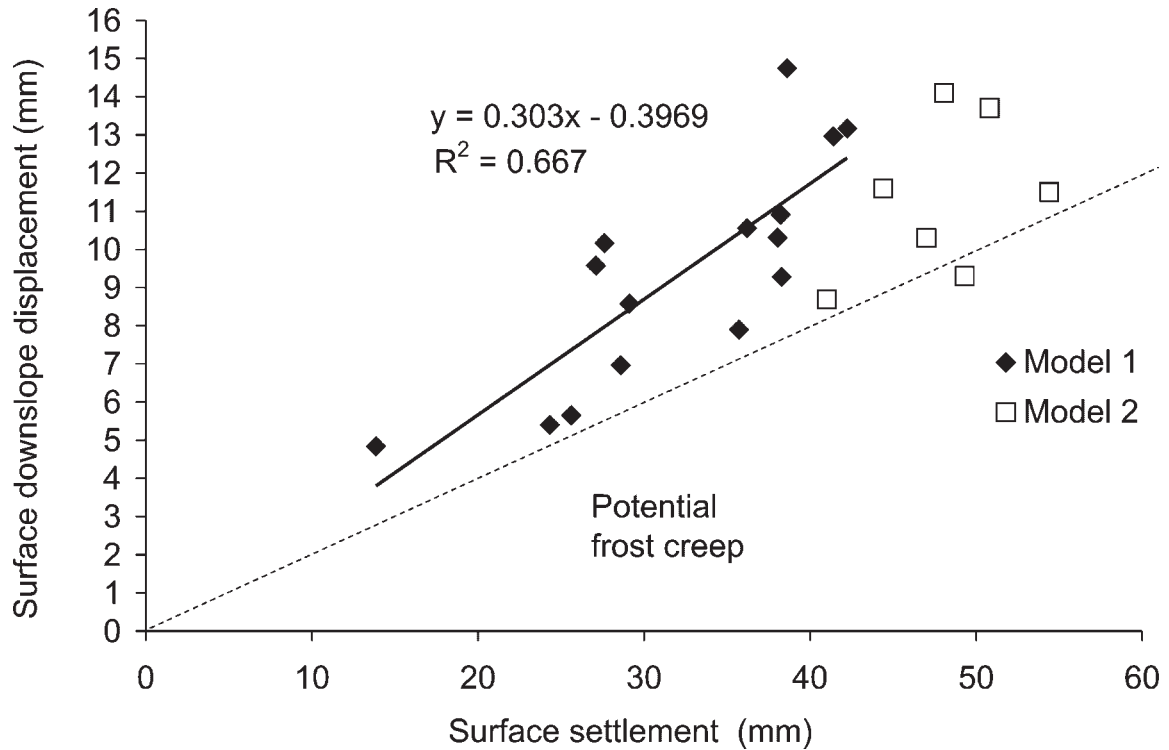


Figure 8 Surface settlement plotted against downslope surface movement. Dashed line shows displacements arising from potential creep (frost heave and vertical resettlement). Note that 16 cycles are included for Model 1, but only cycles ten to 16 for Model 2, representing the period during which the basal freezing plate functioned correctly and provided a uniform permafrost table.

similar to that of the one-sided freezing model (Model 1) than the remaining two-sided freezing cycles in Model 2.

Previous one-sided freezing simulation experiments have suggested that for a given slope gradient there is a positive correlation between surface thaw settlement and surface downslope movements (Harris *et al.*, 1995, 2003), and this was the case here (Figure 8). In Model 2 the range of heave values was insufficient to derive a significant correlation, but downslope displacement/surface settlement ratios were similar to Model 1 (Figure 8). The maximum potential soil creep has been assumed to correspond with vertical soil resettlement during thaw (Washburn, 1967), and this was exceeded in all thaw cycles in both models, except cycle 13 in Model 2 (Figure 8).

#### The Depth Distribution of Soil Shear Strain

Thermistor probe data provided the time when soil thawing was complete (end of the zero curtain) at

progressively greater depths in the soil. By attributing surface downslope displacement measured over any arbitrary time period (say between time (a) and time (b)) to shear strain within the layer of soil that thawed over the same time interval, the distribution of shear deformation through the soil profile was reconstructed for each thaw cycle. Assuming surface settlement between time (a) and time (b) was also generated by consolidation of the soil layer that thawed over that time interval, thaw settlement amounts were also determined for each successive depth increment. Plotting shear strain (differential movement between the top and bottom of the thawing layer divided by the unfrozen thickness of the layer) against axial strain (thaw settlement within the thawing soil layer divided by the unfrozen thickness) for all layers over all cycles (cycles one to 16) for the one-sided freezing model (Model 1) shows a strong linear relationship (Figure 9a). In the two-sided freezing permafrost model (Model 2), shear strain at the base varied considerably, mainly in response to changes in ice content at the base of the active layer between cycles.

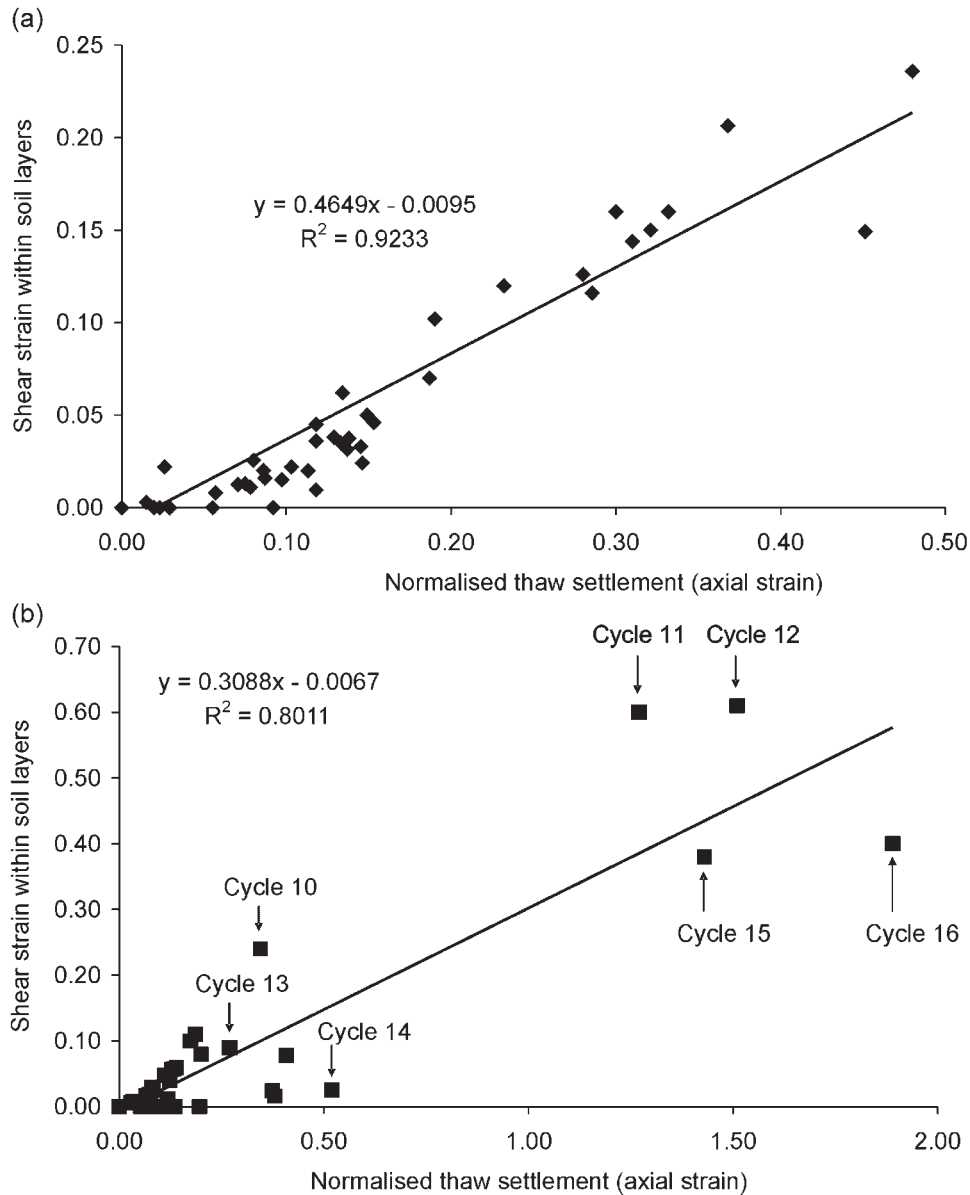


Figure 9 Scatter graphs of shear strain within successive soil layers against normalised thaw settlement (axial strain = change in thickness/final thickness) within the corresponding soil layer. (a) Model 1. (b) Model 2. Shear strains within the basal ice-rich zone are labelled.

Basal shear strain/axial strain values are arrowed in Figure 9b. Clearly, cycles 11, 12, 15 and 16 had axial strains caused by thaw settlements that were much greater than at any depth in the overlying active layer, and much greater than those observed at any depth in Model 1. These high values of basal thaw settlement in Model 2 occurred within a layer of unfrozen thickness around 50 mm, and are reflected in high average heaving ratios observed at this depth in (see Table 2).

### Profiles of Soil Movement

Accumulating shear deformation calculated for the successive soil layers defined above allowed us to calculate synthetic movement profiles for each thaw cycle (Figure 10). Profiles from each of the final eight freeze-thaw cycles in the experimental series were accumulated and compared with adjacent excavated Rudberg columns that were in place over the same

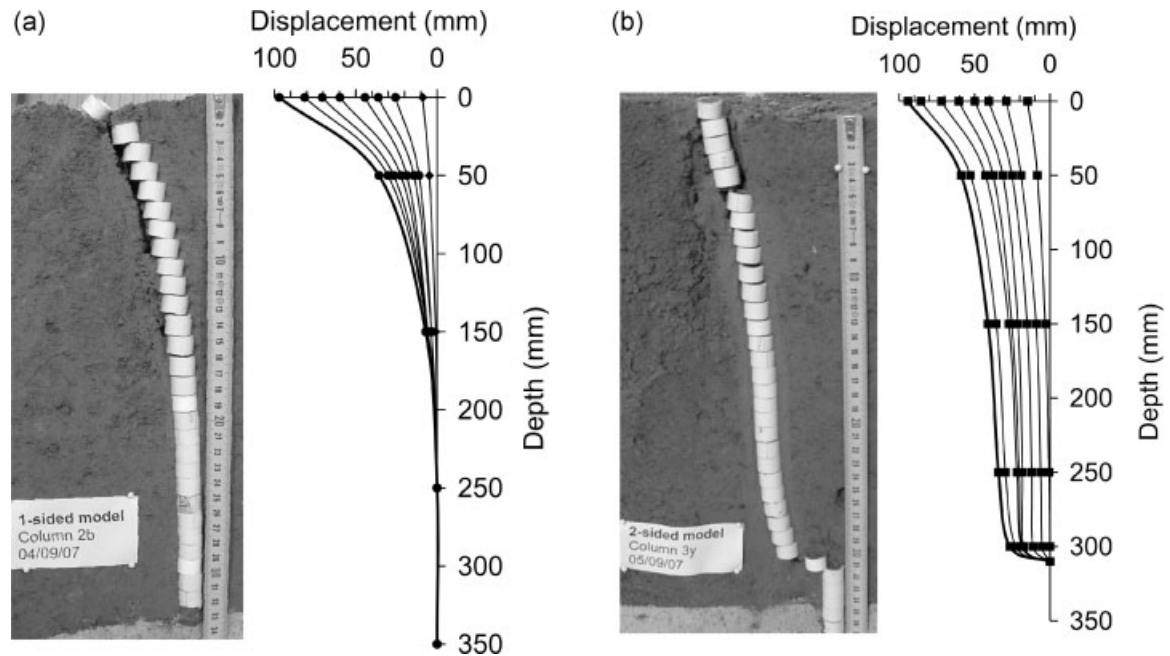


Figure 10 Excavated Rudberg columns compared with synthetic displacement profiles accumulated through freeze-thaw cycles nine to 16. (a) Model 1 (one-sided freezing). (b) Model 2 (two-sided freezing).

sequence of thermal cycles (Figure 10). Patterns of shear strain were closely replicated, though near-surface shearing in Model 2 was slightly over-estimated and basal shear slightly underestimated.

It is clear that the upper part of the active layer in Model 2 responded in a similar way to the one-sided freezing model, but high ice contents in the basal zone immediately above the permafrost table caused extremely high shear strain in most cycles.

### Pore Water Pressures

Pore pressure transducers were located at depths of 50, 150 and 250 mm in the one-sided freezing model (Model 1) and 150, 250 and 300 mm in the two-sided freezing model (Model 2). During the experiment however, some transducers were damaged, or their performance was compromised by air entry during periods when the soil was dry, so that only a partial record of pore pressure variation is available. In Model 1 the 250 mm transducer failed to function correctly following cycle eight in the overall 16 cycle series, while in Model 2, only cycle 14 had a satisfactory record from all three transducers. Variation in pore pressures recorded by a given transducer during

successive freeze-thaw cycles suggests that transducers were strongly influenced by local ice content, which varied from cycle to cycle.

Figure 11a and 11b shows pore pressure variation during thawing of Model 1 in cycle five, which closely resembled that observed during earlier physical modelling experiments, both at full scale (Harris *et al.*, 1995) and in scaled centrifuge simulations (Harris *et al.*, 2003, 2008a). Heaving (ice) pressures developed in the frozen soil at depths of 150 mm and 250 mm, but not at 50 mm. During penetration of the thaw plane, ice pressure fell rapidly and during the zero curtain when the soil was partially thawed, pore pressures were negative. Immediately thawing at the depth of the transducer was complete, pore pressures rose, though at 50 mm they remained negative. In contrast, pressure at 150 mm and 250 mm rose to +2 kPa and +1.4 kPa, respectively. Equivalent hydrostatic pressures (with water table at the surface) were 1.4 kPa and 2.4 kPa, respectively, so that pore pressures at 15 cm depth exceeded hydrostatic for a period of 27 h. Through much of the thaw phase, the pressure gradient behind the thaw plane was in excess of hydrostatic, indicating upward seepage.

Similar pore pressure variations at 50 mm and 150 mm depths were recorded in later cycles, a typical

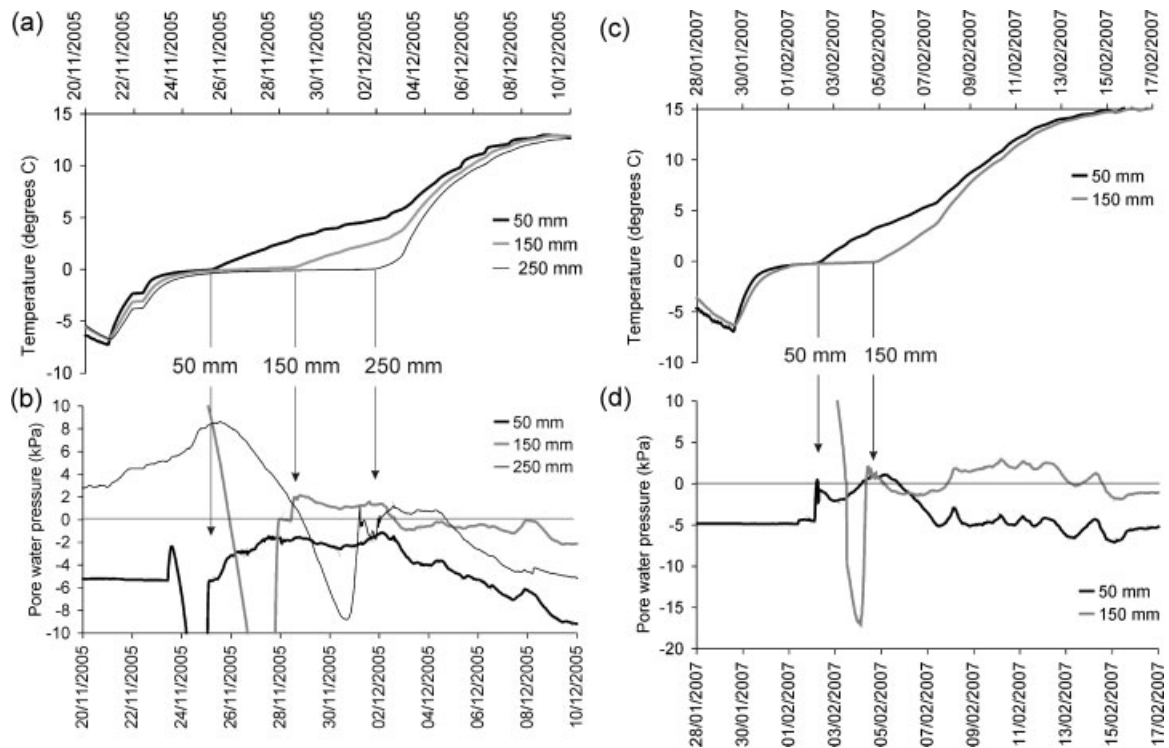


Figure 11 Pore pressures and soil temperatures recorded during thaw in Model 1. (a) Cycle five, soil temperatures. (b) Cycle five, pore water pressures. (c) Cycle 13, soil temperatures. (d) Cycle 13, pore water pressures. Arrows indicate when temperatures rose above zero at each transducer depth.

example being cycle 13 (Figure 11c and 11d). Again negative pore pressures were observed during the zero curtain, followed by a sharp rise following complete thaw. During consolidation an upward hydraulic gradient developed. Falling pore pressures following the post-thaw maximum were followed by a further rise in response to upward seepage from thawing soil lower in the profile.

In Model 2, cycle 14 recorded heaving (ice) pressure in the 250 mm transducer, and briefly, immediately prior to final thawing, at 150 mm depth, possibly associated with refreezing of percolating meltwater (see Harris *et al.*, 2008c). Following complete thaw, all transducers registered a rise in pore pressures, at 150 mm to 0.8 kPa, at 250 mm to 1.7 kPa and at 300 mm to 4.8 kPa (Figure 12). Equivalent hydrostatic pressures at these depths are 1.5, 2.4 and 2.9, so that pore pressures in excess of hydrostatic were generated at 250 mm and 300 mm. Upward hydraulic gradients in excess of hydrostatic associated with high basal pore pressure would have driven upward seepage of meltwater, generating seepage pressures.

## DISCUSSION

### Movement Rates and Patterns

The experiments described above provide generic models of solifluction on two identical slopes in which contrasting thermal regimes led to distinctly different ice distributions. In the one-sided freezing model, representing seasonally frozen terrain with no permafrost, movement profiles were concave down-slope, with maximum shear strain close to the surface. Profiles closely resemble previous laboratory simulations that used similar silty, non-cohesive test soils at full scale (Coutard *et al.*, 1988; Harris *et al.*, 1993, 1996), and at reduced scale in the geotechnical centrifuge (Harris *et al.*, 2003; Kern-Luetsch *et al.*, 2008). Similar movement profiles are also reported in field studies (e.g. Williams, 1966; Price, 1973; Harris, 1981; Kinnard and Lewkowicz, 2005; Harris *et al.*, 2008c). Centrifuge experiments have, however, suggested that the zone of maximum shear may be lower in the profile in more cohesive clay-rich soils (Harris *et al.*, 2008a).

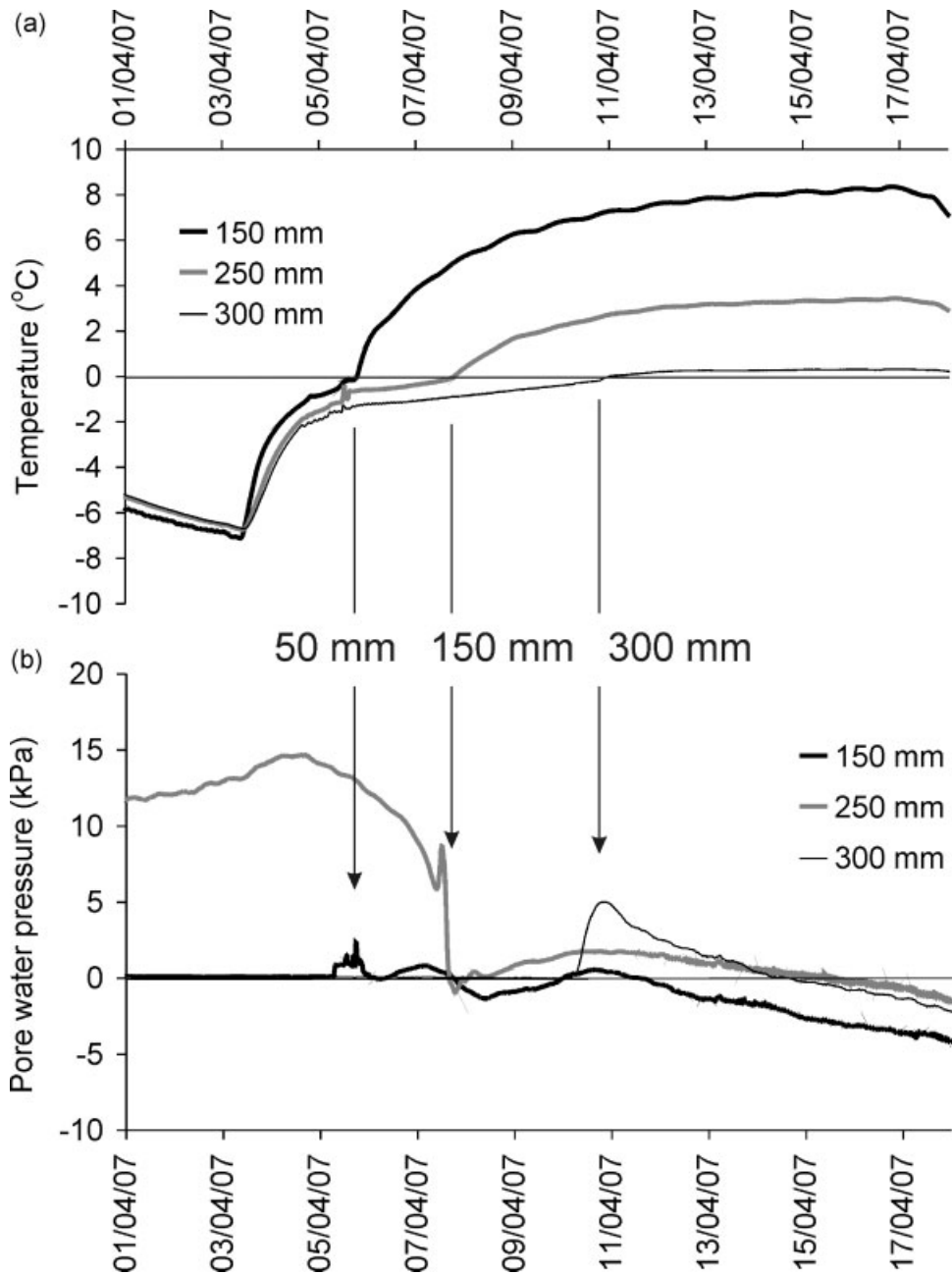


Figure 12 Pore pressures and soil temperatures recorded during thaw in Model 2 cycle 14. (a) Soil temperatures. (b) Pore water pressures. Arrows indicate when temperatures rose above zero at each transducer depth.

The two-sided freezing model, simulating a seasonally thawed active layer above a permafrost table, successfully generated the 'plug-like' solifluction movements first described by Mackay (1981) and reported by Lewkowicz and Clarke (1998) and

Matsuoka and Hirakawa (2000) in which shear strain is concentrated in the active layer basal ice-rich zone. Field monitoring in Svalbard during summer 2006, when thawing penetrated the ice-rich layer at the base of the active layer and in the top of the permafrost,

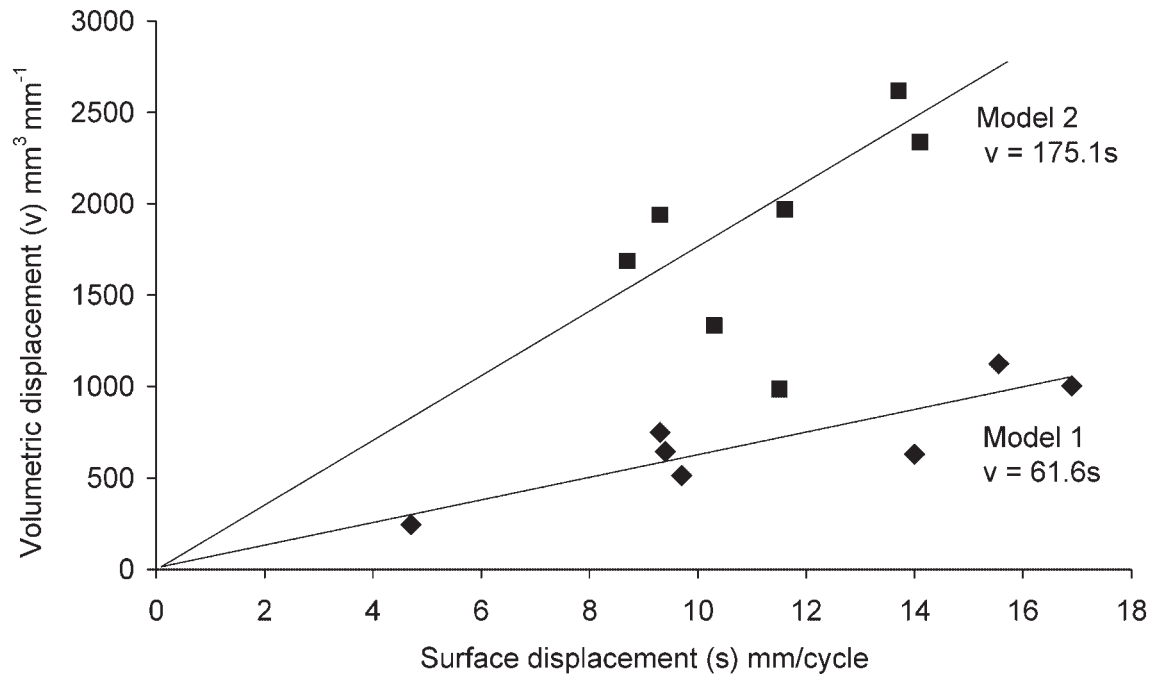


Figure 13 Relationship between surface movement and volumetric transport, Model 1 (one-sided freezing, no permafrost) and Model 2 (two-sided freezing with permafrost).  $V$  = volumetric transport rate ( $\text{mm}^3 \text{mm}^{-1}$ );  $s$  = surface displacement rate  $\text{mm cycle}^{-1}$ ).

showed timing of solifluction movements and distribution of shear strain almost identical with that observed in Model 2, with little thaw settlement and shear deformation within the ice-poor central parts of the active layer, and maximum shear strain within the basal zone where thaw consolidation was extreme (Harris *et al.*, 2006).

Rates of simulated soil movements fell within those observed in the field, with surface rates in Model 1 (seasonally frozen) ranging from 5 mm per cycle to 15 mm per cycle (mean 9.5 mm per cycle), and in Model 2 (permafrost) ranging from 9 mm per cycle to 14 mm per cycle (mean 11.5 mm per cycle). Soil transport rates, measured as volume of soil passing through a unit width of slope per cycle (termed volumetric velocity by Matsuoka, 2001, who used units of  $\text{cm}^3 \text{cm}^{-1}$ ) ranged from  $2.4 \text{cm}^3 \text{cm}^{-1}$  per cycle to  $11.2 \text{cm}^3 \text{cm}^{-1}$  per cycle in Model 1, with mean  $7 \text{cm}^3 \text{cm}^{-1}$  per cycle, and from  $9.9 \text{cm}^3 \text{cm}^{-1}$  per cycle to  $26.2 \text{cm}^3 \text{cm}^{-1}$  per cycle in Model 2, with mean  $18.4 \text{cm}^3 \text{cm}^{-1}$  per cycle. Rates are low compared with field values (see Matsuoka, 2001), because the thicknesses of the laboratory profiles (350 mm Model 1 and 310 mm Model 2) were less than commonly observed in the field.

Matsuoka (2001) reported much greater volumetric transport in permafrost regions where solifluction

shear strains are concentrated in the base of the active layer compared with non-permafrost regions, and this is highlighted here. Volumetric transport per unit of surface displacement in Model 2 was more than 2.8 times greater than in Model 1 (Figure 13), emphasising the potential significance of solifluction processes to long-term slope evolution in permafrost regions. Similar differences in volumetric soil transport were observed in scaled centrifuge modelling experiments by Kern-Luetsch *et al.* (2008). The variability in volumetric transport within the Model 2 data set reflects variable amounts of ice segregation within the basal zone of the active layer between successive freezing and thawing cycles, giving variable amounts of basal shear strain. This is probably replicated in many field sites.

### Significance of Pore Water Pressures

Considerable pore pressure variation between cycles was observed in both models at all depths. Similar variability has been observed in full-scale simulation experiments (e.g. Harris *et al.*, 1997) and in reduced scale centrifuge modelling (Harris *et al.*, 2003, 2008a). Simple stability analysis based on an infinite planar slope model (Skempton and DeLory, 1957)

assumes both shear surface and water seepage parallel to the ground surface, and gives a Factor of Safety of:

$$F_s = \frac{c' + z(\gamma - m\gamma_w) \cos^2 \beta \tan \phi'}{z\gamma \sin \beta \cos \beta} \quad (1)$$

where  $\gamma$  is bulk unit weight of the thawing soil,  $\gamma_w$  is the unit weight of water,  $z$  is the depth of the potential slip surface,  $m$  is the ratio of the height of the piezometric surface above the slip surface to the vertical depth of the slip surface below the ground surface,  $\beta$  is slope angle and  $\phi'$  is the internal angle of friction of the soil. The variation in pore pressure may be summarised by plotting maximum pore pressure recorded in a given thaw cycle against depth of transducer (Figure 14). This analysis suggests that while the majority of measured pore pressures were below the critical value for slope failure, some exceeded this threshold. No slope failure was observed, possibly reflecting localised pressure variations that were insufficiently widespread across the model to promote landsliding. In the case of Model 2, the toe zone extended beyond the basal freezing plate

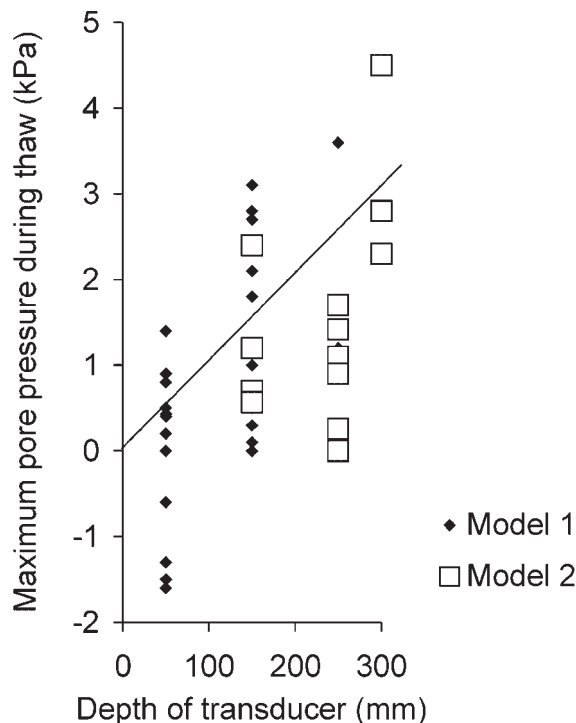


Figure 14 Maximum recorded pore pressures plotted against depth of transducer. Line shows pore pressure-depth relationship for Factor of Safety = 1 based on the infinite slope model (see text).

and undoubtedly provided buttressing of the slope by increasing forces resisting failure.

Seepage pressures generated by upward hydraulic gradients driving meltwater upward through the soil, away from the thaw front, are not considered in the above analysis, but would have contributed to the reduction in effective stress within these thawing soils (see Harris, 2008a).

### Landscape Development

The model results have some important implications to understanding of periglacial hillslope development. Where the substrate is frost-susceptible non-cohesive soil and sufficient moisture is available for ice segregation, sediment transport by solifluction is likely to be substantially greater in cold permafrost regions than in either warm permafrost or in non-permafrost regions. Solifluction will be favoured by melt of larger volumes of segregated ice, in the extreme by complete thaw of the ice-rich transient layer, for example during periods of climate warming and permafrost degradation. By implication, the thick sequences of Pleistocene periglacial slope deposits in, for instance, southwest England and northwest France (Ballantyne and Harris, 1994; Bates *et al.*, 2003) may preferentially record shorter phases of cold and moist permafrost (e.g. during some parts of Marine Isotope Stages 4 and 2) and/or permafrost degradation (e.g. during Greenland Interstadials 2 and 1e), or they may reflect longer phases of warm permafrost or just seasonal frost (e.g. during Marine Isotope Stage 3), or a combination of conditions. Optical luminescence dating of interbedded silty or sandy layers – attributed to slopewash and therefore potentially exposed to sunlight during deposition – might discriminate between them.

### CONCLUSIONS

The experimental procedures reported here have addressed three major hypotheses. Firstly, that significant differences occur in ice distribution and timing of frost heaving and resettlement between slopes with seasonally frozen ground (one-sided freezing) and those underlain by a seasonally thawed active layer above cold permafrost (two-sided freezing). In the present experiments frost heaving was only observed through the period of winter frost penetration during the one-sided freezing (Model 1) and soil ice content decreased with depth. In contrast, summer frost heaving occurred late in each thaw phase in the modelled active layer (Model 2), as a result of

simulated summer rainfall percolating to the permafrost table and this was followed by a second phase of frost heaving concentrated near the lower and upper boundaries as the active layer refroze from the top down and from the permafrost table upwards. Segregation ice in Model 2 was concentrated at the base of the model and also near the surface, with a relatively ice-poor region in mid profile. Thus, the thermal regime is shown to strongly influence both frost heave and ice distribution.

The second hypothesis considered here was that solifluction profiles reflect differences in ice distribution. Our experiments were able to demonstrate that solifluction-induced shear strain occurred during thaw and was closely related to zones with high thaw consolidation, which in turn were determined by the distribution of segregation ice. Profiles of soil movement showed marked contrasts, with shear strain concentrated near the surface in the one-sided freezing model (Model 1), but at the base of the active layer, immediately above the permafrost table in Model 2. Therefore, in cold permafrost areas with two-sided active layer freezing and high basal ice contents, the active layer effectively moves downslope *en masse* with surface displacement rates only a little greater than basal displacement rates. This results in significantly higher volumetric transport rates for a given rate of surface movement. In the present experiment, volumetric transport was almost three times higher in the two-sided experiment than in the one-sided freezing experiment (seasonally frozen ground) for a given surface movement velocity.

Finally, these experiments investigated the hypothesis that soil deformation was associated with increased pore water pressures generated by thaw consolidation, with higher pore pressures in zones of greater thaw consolidation. Data showed that pore pressures varied between freezing and thawing cycles, but were significantly raised during thaw consolidation in ice-rich zones, leading to a reduction in effective stress and incremental shear deformations. As indicated above, shear strains were in consequence greatest near the surface in Model 1 where thaw consolidation was high, and in the active layer basal zone in Model 2, again where thaw consolidation was high. It appears that in Model 2, pore pressures during basal thawing were sufficiently high to allow large shear strains to develop, but not sufficient to initiate widespread shear failure and shallow landsliding.

Scaled centrifuge modelling of solifluction processes associated with one-sided and two-sided freezing, using geometrically similar slope models to our full-scale simulations, and constructed of the same test soil, have yielded results highly consistent

with those presented here (Kern-Luetschg and Harris, 2008; Kern-Luetschg *et al.*, 2008). Field validation of both physical modelling approaches (full scale and centrifuge) is currently in process (Harris *et al.*, 2006, 2007, 2008c), and field and laboratory data will be used in the development and testing of new numerical approaches to predicting the geotechnical behaviour of thawing ice-rich soil (Cleall *et al.*, 2006; Thomas *et al.*, submitted).

## ACKNOWLEDGEMENTS

This research was funded by the British Natural Environment Research Council (Grant NER/B/S/2003/00748) and the British Engineering and Physical Sciences Research Council Research Grant GR/T22964. Laboratory assistance from Gerard Guilmet and Anthony Dubois is gratefully acknowledged.

## REFERENCES

- Ballantyne CK, Harris C. 1994. *The Periglaciation of Great Britain*. Cambridge University Press: Cambridge.
- Bates MR, Keen DH, Lantieri J-P. 2003. Pleistocene marine and periglacial deposits of the English Channel. *Journal of Quaternary Science* **18**: 319–337.
- Benedict JB. 1970. Downslope soil movement in a Colorado alpine region: rates, processes, and climatic significance. *Arctic and Alpine Research* **2**: 165–226.
- Cheng G. 1983. The mechanism of repeated segregation for the formation of thick-layered ground ice. *Cold Regions Science and Technology* **8**: 57–66.
- Cleall PJ, Thomas HR, Glendinning MC. 2006. Modelling the behaviour of freezing and thawing soil slopes. In *Proceedings 5th International Congress on Environmental Geotechnics*, (5th ICEG) Cardiff, UK, 26–30 June, Vol. 2, 1603–1610.
- Coutard J-P, Van Vliet-Lanoe B, Auzuet AV. 1988. Frost heaving and frost creep on an experimental slope: results for soil structures and sorted stripes. *Zeitschrift für Geomorphologie, Supplementband* **71**: 13–23.
- Harris C. 1981. *Periglacial Mass Wasting: A Review of Research*. BGRG Research Monograph. Geo Books: Norwich.
- Harris C. 1996. Physical modelling of periglacial solifluction: review and future strategy. *Permafrost and Periglacial Processes* **7**: 349–360.
- Harris C, Davies MCR. 2000. Gelifluction: observations from large-scale laboratory simulations. *Arctic, Antarctic and Alpine Research* **32** No 2: 202–207.
- Harris C, Gallop M, Coutard J-P. 1993. Physical modelling of gelifluction and frost creep: some results of a large-scale simulation experiment. *Earth Surface Processes and Landforms* **18**: 383–398.

- Harris C, Davies MCR, Coutard J-P. 1995. Laboratory simulation of periglacial solifluction: significance of porewater pressure, moisture contents and undrained shear strength during thawing. *Permafrost and Periglacial Processes* **6**: 293–312.
- Harris C, Davies MCR, Coutard J-P. 1996. An experimental design for laboratory simulation of periglacial solifluction processes. *Earth Surface Processes and Landforms* **21**: 67–75.
- Harris C, Davies MCR, Coutard J-P. 1997. Rates and processes of periglacial solifluction: an experimental approach. *Earth Surface Processes and Landforms* **22**: 849–868.
- Harris C, Rea BR, Davies MCR. 2000. Geotechnical centrifuge modelling of gelification processes: validation of a new approach to periglacial slope studies. *Annals of Glaciology* **31**: 263–268.
- Harris C, Rea BR, Davies MCR. 2001. Scaled physical modeling of mass movement processes. *Permafrost and Periglacial Processes* **12**: 125–136. DOI: 10.1002/ppp.373
- Harris C, Davies MCR, Rea B. 2002. Centrifuge modelling of slope processes in thawing ice-rich soils. In *Physical Modelling in Geotechnics: Proceedings International Conference on Physical Modelling in Geotechnics*, Phillips R, Guo PJ, Popescu R (eds). St John's Newfoundland, July 2002. Swets and Zeitlinger: Lisse; 297–302.
- Harris C, Davies MCR, Rea BR. 2003. Gelification: viscous flow or plastic creep? *Earth Surface Processes and Landforms* **28**: 1289–1301.
- Harris C, Luetschg M, Murton JB, Smith FW, Davies MCR, Christiansen HH, Ertlen-Font M. 2006. Solifluction Processes in Arctic Permafrost: Results of Laboratory and Field Experiments. *Eos Trans. AGU*, **87**(52): Fall Meeting Supplement, Abstract C43A-03.
- Harris C, Luetschg M, Davies MCR, Smith F, Christiansen HH, Isaksen K. 2007. Field instrumentation for real-time monitoring of periglacial solifluction. *Permafrost and Periglacial Processes* **18**: 105–114. DOI: 10.1002/ppp.573
- Harris C, Smith JS, Davies MCR, Rea B. 2008a. An investigation of periglacial slope stability in relation to soil properties based on physical modelling in the geotechnical centrifuge. *Geomorphology* **93**: 437–459.
- Harris C, Kern-Luetschg M, Murton J, Font M, Davies MCR, Smith F. 2008b. Full-scale physical modeling of solifluction processes associated with one-sided and two-sided active layer freezing. In *Ninth International Conference on Permafrost*, Kane DL, Hinkel KM (eds). Institute of Northern Engineering, University of Alaska Fairbanks; 663–668.
- Harris C, Kern-Luetschg MA, Smith FW, Isaksen K. 2008c. Solifluction processes in an area of seasonal ground freezing, Dovrefjell, Norway. *Permafrost and Periglacial Processes* **19**: 31–47. DOI: 10.1002/ppp.609
- Higashi A, Corte AE. 1971. Solifluction: a model experiment. *Science* **171**: 480–482.
- Jaesche P, Veit H, Huwe B. 2003. Snow cover and soil moisture controls on solifluction in an area of seasonal frost, eastern Alps. *Permafrost and Periglacial Processes* **14**: 399–410. DOI: 10.1002/ppp.471
- Journaux A, Coutard J-P. 1976. Recherches et expérimentations. *Centre de Géomorphologie, Bulletin*, **21**: 13–28.
- Kern-Luetschg M, Harris C. 2008. Centrifuge modelling of solifluction processes: displacement profiles associated with one-sided and two-sided active layer freezing. *Permafrost and Periglacial Processes* **19**: 379–392. DOI: 10.1002/ppp.633
- Kern-Luetschg M, Harris C, Cleall P, Li Y, Thomas H. 2008. Scaled centrifuge modeling in permafrost and seasonally frozen soils. In *Ninth International Conference on Permafrost*, Kane DL, Hinkel KM (eds). Institute of Northern Engineering, University of Alaska Fairbanks; 919–924.
- Kinnard C, Lewkowicz AG. 2005. Movement, moisture and thermal conditions at a turf-banked solifluction lobe, Kluane Range, Yukon Territory, Canada. *Permafrost and Periglacial Processes* **16**: 261–275.
- Lewkowicz AG. 1988. Slope processes. In *Advances in Periglacial Geomorphology*, Clark MJ (ed.). Wiley: Chichester; 325–368.
- Lewkowicz AG, Clarke S. 1998. Late summer solifluction and active layer depths, Fosheim Peninsula, Ellesmere Island, Canada. In *Proceedings the Seventh International Conference on Permafrost, 23–27 June 1998, Yellowknife, Canada*, Lewkowicz AG, Allard M (eds). Nordicana, Centre d'études nordiques: Québec City; 641–646.
- Mackay JR. 1981. Active layer slope movement in a continuous permafrost environment, Garry Island, Northwest Territories, Canada. *Canadian Journal of Earth Sciences* **18**: 1666–1680.
- Mackay JR. 1983. Downward water movement into frozen ground, western Arctic coast, Canada. *Canadian Journal of Earth Sciences* **20**: 120–134.
- Matsuoka N. 2001. Solifluction rates, processes and landforms: a global review. *Earth-Science Reviews* **55**: 107–134.
- Matsuoka N, Hirakawa K. 2000. Solifluction resulting from one-sided and two-sided freezing: field data from Svalbard. *Polar Geoscience* **13**: 187–201.
- McRoberts EC, Morgenstern NR. 1974. The stability of thawing slopes. *Canadian Geotechnical Journal* **11**: 447–469.
- Price LW. 1973. Rates of mass-wasting in the Ruby Range, Yukon Territory. In *North American Contribution, 2<sup>nd</sup> International Conference on Permafrost, Yakutsk*. National Academy of Sciences: Washington; 235–245.
- Rein RG, Burrous CM. 1980. Laboratory measurements of subsurface displacement during thaw of low-angle slopes of frost-susceptible soil. *Arctic and Alpine Research* **12**: 349–358.
- Shiklomanov NI, Nelson F. 2007. Active layer processes. In *Encyclopedia of Quaternary Science*, 13, Elias SA (ed.). Elsevier: Oxford; 2138–2146.

- Shur YI. 1988. The upper horizon of permafrost soils. In *Proceedings of the Fifth International Conference on Permafrost*, Senneset K (ed.). Tapir: Trondheim; 867–871.
- Shur Y, Hinkel KM, Nelson FE. 2005. The transient layer: implications for geocryology and climate-change science. *Permafrost and Periglacial Processes* **16**: 5–17.
- Skempton AW, DeLory FA. 1957. Stability of natural slopes in London Clay. In *Proceedings of the 4th International Conference on Soil Mechanics*, 2, 378–381.
- Smith DJ. 1988. Rates and controls of soil movement on a solifluction slope in the Mt Rae area, Canadian Rocky Mountains. *Zeitschrift für Geomorphologie, Supplementband* **71**: 25–44.
- Washburn AL. 1967. Instrumental observations of mass-wasting in the Mesters Vig district. *Northeast Greenland. Meddelelser om Grønland* **166**: 318pp.
- Washburn AL. 1979. *Geocryology: a Survey of Periglacial Processes and Environments*. Edward Arnold: London.
- Williams PJ. 1966. Downslope soil movement at a Sub-Arctic location with regard to variations in depth. *Canadian Geotechnical Journal* **3**: 191–203.